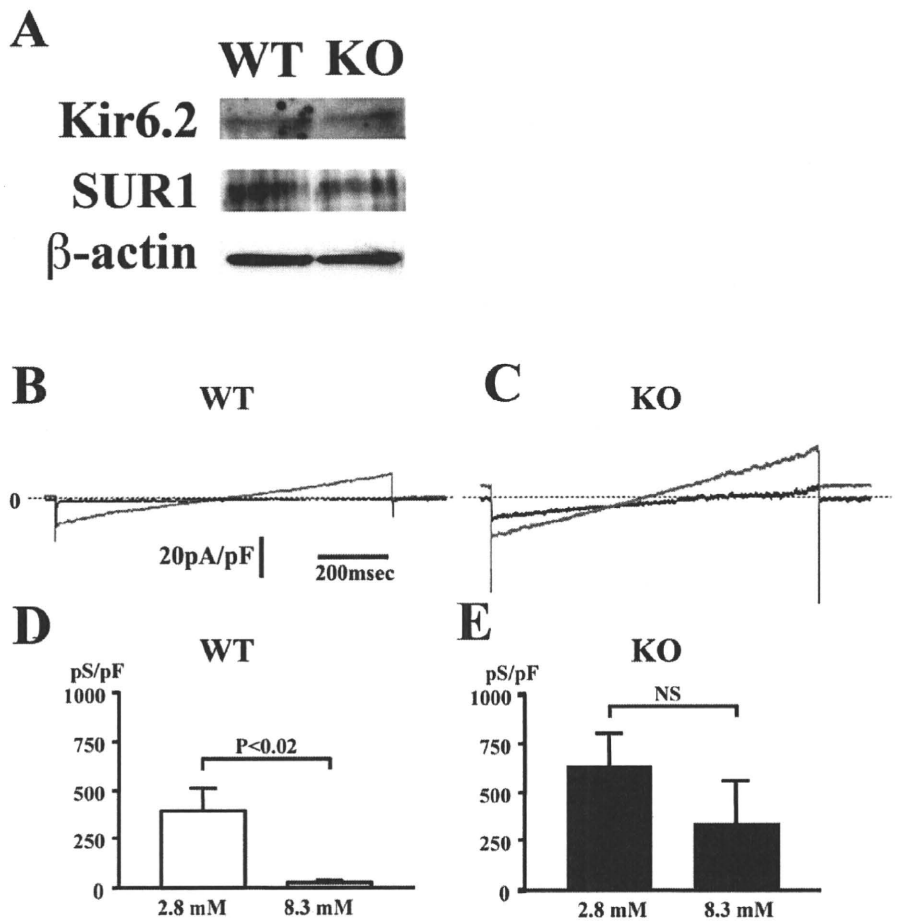

Figure 6. Effects of the increase in glucose concentration on K_{ATP} channel currents in WT and *CDKAL1* KO β-cells. A. Expression of Kir6.2 and SUR1 proteins in WT and KO islets by immunoblotting. Equal amounts of islet protein (30 μg) were separated by SDS-PAGE and immunoblotted. β-actin was used as a loading control. **B–E.** K_{ATP}-channel currents expressed as current density in the ramp-clamp mode between −100 mV and −50 mV at a rate of 0.5 mV/ms in the presence of 2.8 mM (red line) or 8.3 mM glucose (black line) in WT (**B** and **D**) and KO β cells (**C** and **E**). Dotted lines indicate 0 A. Results are means±SEM and paired t-test was used to compare the data.
doi:10.1371/journal.pone.0015553.g006

(TMRE). Hyperpolarization of the mitochondrial membrane potential is evident by an increase in the fluorescent intensity of TMRE [15]. *CDKAL1* KO cells exhibited a significantly reduced membrane potential response to glucose stimulation compared with WT cells (Fig. 7B). The reduced mitochondrial membrane potential response was further confirmed using α-ketoisocaproate (KIC) (Fig. 7C), which is a direct substrate for the mitochondrial TCA cycle and bypasses glycolysis [16]. Thus, it seems reasonable to conclude that the defective ATP generation in KO cells is due to impaired mitochondrial function, without changes in mitochondrial number or morphology in KO cells on electron microscopy (data not shown).

CDK5/p35 protein kinase activity in *CDKAL1* KO islets

CDKAL1 is homologous to CDK5RAP1, which inhibits CDK5 activity by binding to the kinase activator p35 [6]. To test whether CDK5-mediated regulation is involved in the function of CDKAL1 in β cells, we examined the expression and protein kinase activity of CDK5 in *CDKAL1* KO islets. CDK5 and p35 were expressed in KO islets as much as in WT islets (Fig. 8A). Surprisingly, we found no difference in CDK5/p35 kinase activity between *CDKAL1* KO and WT islets, when using histone H1 as a substrate after immunoprecipitation with a p35-specific antibody (Fig. 8B). The specificity of this activity was confirmed using the CDK5 inhibitor roscovitine. Thus, it seems likely that CDK5 kinase does not contribute to CDKAL1 function in β cells.

Subcellular localization of CDKAL1 in β cells

Finally, we examined the subcellular localization of CDKAL1 using a biochemical subcellular fractionation of MIN6 β cells. In the fractionation procedure [17], the postnuclear S1 fraction was separated by differential centrifugation into an S2 soluble cytosolic/microsomal fraction and a pellet membrane fraction. Then, the S2 fraction was separated into the S3 soluble cytosolic fraction. Endogenous proteins were used as markers for cytosolic (MEK-1/2), endoplasmic reticulum (ER) (BIP/GRP78), mitochondrial (Bcl2), and plasma membrane proteins (SNAP25). CDKAL1 immunoreactivities were detected in the S2 and pellet fractions, but not in the S3 soluble cytosolic fraction (Fig. 9A), suggesting that CDKAL1 seems to associate with microsomes or plasma membrane.

We next performed immunocytochemistry to confirm the subcellular localization of CDKAL1 in β cells. The CDKAL1 antibody cross-reacted with a non-specific protein band (Fig. 1B

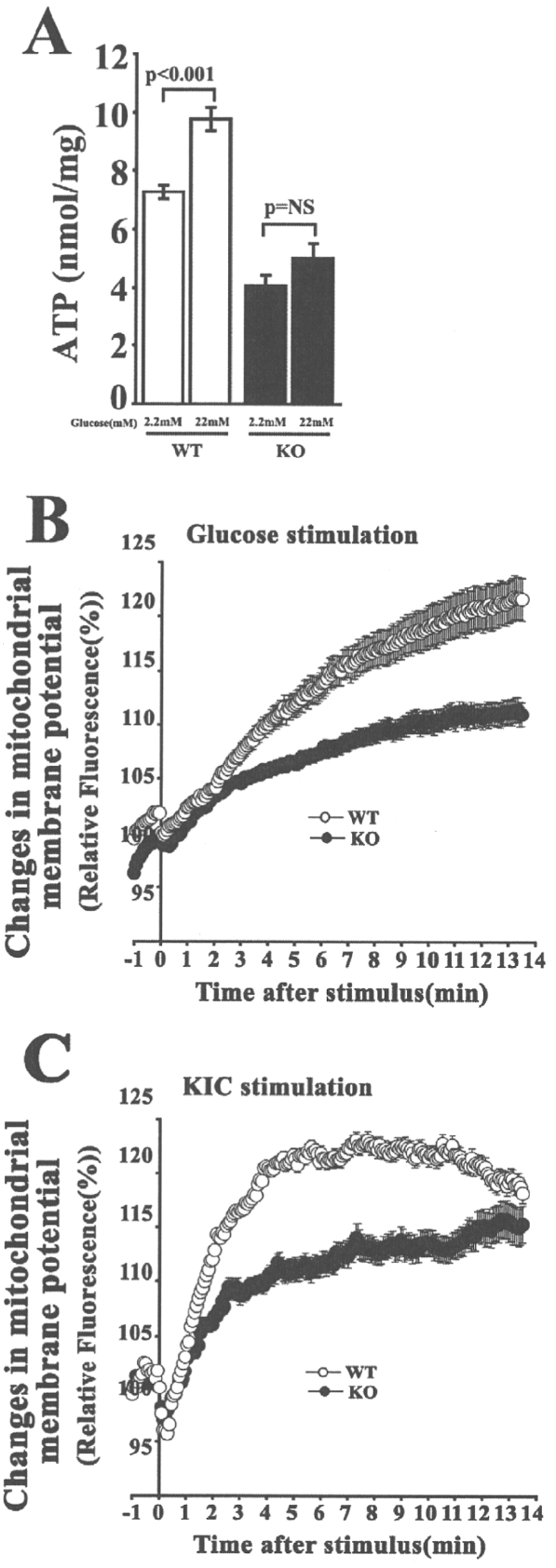

Figure 7. Effects of *CDKAL1* KO on ATP generation. A. ATP content in WT and *CDKAL1* KO islets. HPLC was used to measure ATP content in islets from WT and KO mice after incubation with 2 or 22 mM glucose. Results are means±SEM (n = 7 per group). **B, C.** Changes in mitochondrial membrane potential in response to 22 mM glucose (**B**) and 10 mM KIC (**C**) in WT and KO β cells. Changes in mitochondrial membrane potential were measured by a mitochondrial potential sensitive dye TMRE (10 nM). Time 0 indicates when the stimulants were added. The fluorescence intensity at time 0 was taken as 100%. Results are means±SEM (n = 12 cells per group).
doi:10.1371/journal.pone.0015553.g007

and Fig.9A), suggesting that the antibody is not suitable for immunostaining. In fact, in immunostaining experiments with the CDKAL1 antibody, we could not detect any specific signal in WT cells (data not shown). Therefore, we expressed the CDKAL1 protein as a fusion with enhanced green fluorescent protein (EGFP) and the intracellular localization was examined under a confocal microscope immunostaining with organelle markers or with MitoTracker staining. As shown in Fig. 9B, the fluorescence of the CDKAL1–EGFP protein was colocalized with the ER protein calnexin, but not with MitoTracker Red (a mitochondria marker). These results suggest that CDKAL1 is predominantly localized to the ER.

Discussion

In this study, we found that pancreatic β cells from mice null for *CDKAL1*, which was identified as a susceptibility gene for type 2 diabetes in humans, have a reduced first-phase insulin release *in vitro*. TIRF imaging revealed that *CDKAL1* KO caused a marked reduction in the number of fusion events during first-phase release (Fig. 3), but not in second-phase release. The impaired glucose-induced first-phase insulin exocytosis was associated with a delayed and slow increase in $[Ca^{2+}]_i$ during glucose stimulation in KO cells (Fig. 5). This may be due to the blunted responsiveness of K_{ATP} channels to glucose stimulation in KO cells (Fig. 6). Indeed, ATP production in KO cells was low (Fig. 7) and may lead to blunted glucose-induced K_{ATP} channel responsiveness followed by impaired Ca^{2+} channel activity.

The target molecules for CDKAL1 are not yet known, although our data indicate that *CDKAL1* KO influences glucose-induced K_{ATP} channel responsiveness through reduced ATP generation. Since CDKAL1 is similar to CDK5RAP1, we originally speculated that the function of CDKAL1 is mediated by CDK5, and is probably directly associated with increased Ca^{2+} channel activity, as observed in p35 KO mice [8], or with insulin gene expression [7,9]. However, there was no relationship between CDKAL1 and CDK5 in this study. Therefore, CDK5/p35-mediated regulation does not seem to be involved in CDKAL1 regulation of insulin release. Our data suggest that CDKAL1 is instead related to glucose metabolism, which is associated with ATP generation, K_{ATP} channel activity and Ca^{2+} channels activity.

The failure of glucose-induced ATP-generation may be due to defects at several stages of glucose metabolism including cytosolic glycolysis and mitochondrial metabolism. In *CDKAL1* KO cells, the glucose-stimulated mitochondrial membrane potential response was blunted (Fig. 7B). In addition, KIC, which is a direct substrate for the TCA cycle, bypassing glycolysis, also reduced the mitochondrial membrane potential response (Fig. 7C). Therefore, blunted mitochondrial membrane potential response is likely to be a key defect, resulting in a reduced ATP generation, K_{ATP} channel responsiveness and Ca^{2+} channel activity, and eventually leading to impaired insulin granule exocytosis in KO cells. Indeed, it has

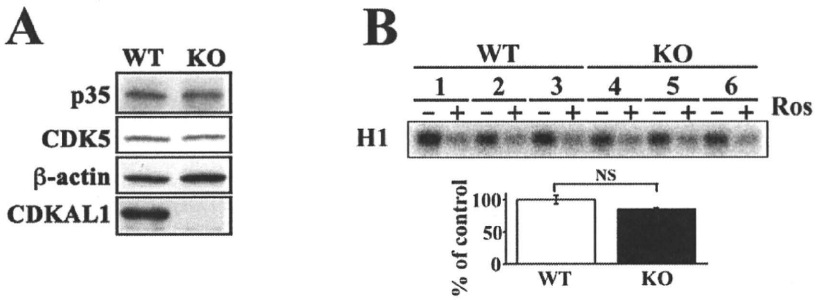

Figure 8. CDK5/p35 protein kinase activity in *CDKAL1* KO islets. A. Detection of CDK5 and p35 proteins in WT and KO islets by immunoblotting. Equal amounts of islet protein (20 μg) were separated by SDS-PAGE and immunoblotted. β-actin was used as a loading control. **B.** Detection of CDK5/p35 kinase activity in WT (lanes 1–3) and KO (lanes 4–6) islets. After immunoprecipitation with a p35-specific antibody in WT and KO islets, kinase activity was measured using histone H1 as the substrate in the presence (+) or absence (−) of a CDK5 inhibitor roscovitine (Ros; 20 μM). Quantification is shown in the lower panel as means±SEM (n = 3 per group).
doi:10.1371/journal.pone.0015553.g008

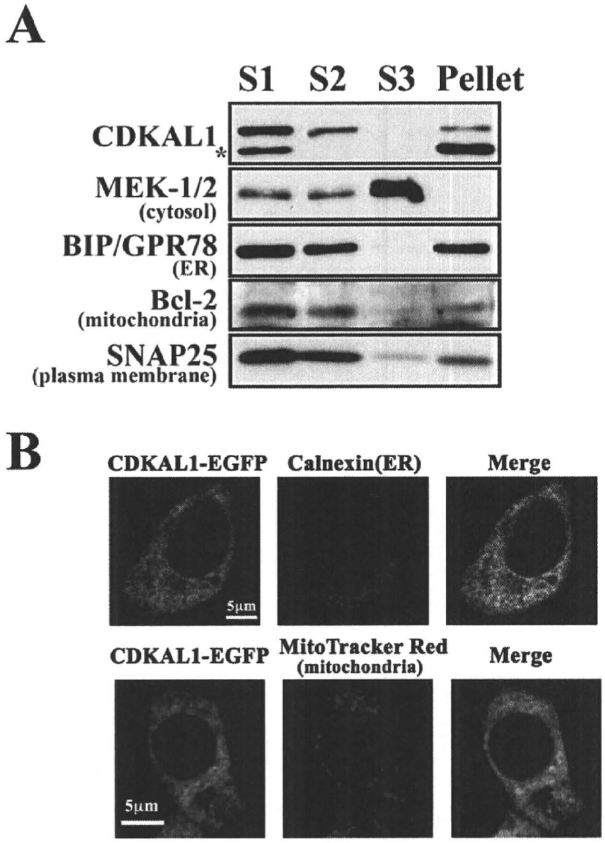

Figure 9. Subcellular localization of CDKAL1 in β cells. A. Subcellular fractionation for CDKAL1 localization. The postnuclear fraction (S1) from MIN6 β cells homogenates was fractionated by differential centrifugation (see Methods). Equal amounts (2 μg protein) of the fractions obtained were analyzed by immunoblotting with the indicated antibodies. S2, soluble cytosolic/microsomal fraction; Pellet, membrane fraction; S3, soluble cytosolic fraction. The protein band below the CDKAL1 protein (*) is a nonspecific protein band detected by the anti-CDKAL1 antibody. **B.** Immunocytochemical localization of CDKAL1 in MIN6 β cells. MIN6 β cells were transfected with EGFP–CDKAL1 and intracellular localization was examined using a confocal microscope with MitoTracker Red staining or immunostaining with anti-calnexin IgG (ER marker), as indicated.
doi:10.1371/journal.pone.0015553.g009

been reported that the selective impairment of glucose-induced insulin release in diabetic Goto-Kakizaki rats is associated with reduced sensitivity of K_{ATP} channels to glucose by deficient oxidative metabolism of glucose in mitochondria [18,19].

In KO cells, cytosolic free $[Ca^{2+}]_i$ induced by glucose gradually reached the same level observed in WT cells. We assume that the increase of $[Ca^{2+}]_i$ during second-phase may reflect suppression of Ca^{2+} clearance mechanism. As for other animal cells, four mechanisms remove Ca^{2+} from cytosol of β cells: sarco-endoplasmic reticulum Ca^{2+}-ATPase (SERCA) pumps, plasma membrane Ca^{2+}-ATPase (PMCA), Na^+/Ca^{2+} exchanger (NCX), and the calcium uniporter of mitochondria [20,21]. In mouse and rat β cells, the SERCA pump is the dominant Ca^{2+} clearance mechanism [20,21], thus it is conceivable that reduced ATP generation impairs the Ca^{2+} clearance function via the SERCA pump, resulting that there is no difference of $[Ca^{2+}]_i$ in second-phase between KO and WT cells.

As shown in Fig. 9, CDKAL1 is likely to localize to the ER in β cells. The relationship between CDKAL1 deletion in the ER and reduced mitochondrial ATP generation remains unknown. However, it has been reported that the ER and mitochondria are in close contact, which supports communication between these two organelles [22]. It is possible that ER dysfunction caused by *CDKAL1* KO may affect mitochondrial function in the KO cells. Such ER–mitochondria communication has been shown to involve the ER stress pathway [22,23], even in β cells [24,25]. Very recently, Arragain et al. reported that CDKAL1 is a methylthiotransferase involved in the biosynthesis of 2-methythio-N6-threonylcarbamoyladenosine in transfer RNA (tRNA) [26]. The methylthio modification of adenosine in tRNA appears to be essential for efficient and highly accurate protein translation by the ER ribosome. However, it is still unclear how the role of CDKAL1 in tRNA may be linked to ER function or ATP generation in mitochondria. Thus, it is tempting to speculate that either ER dysfunction or ER stress may affect the mitochondrial membrane potential in KO cells.

It is particularly interesting to note that our TIRF imaging data showed that CDKAL1 deletion only impaired the first-phase, but not the second-phase, of glucose-induced insulin exocytosis. Our data are in good agreement with the results of Groenewoud et al. [10] and Stancakova et al. [11], who reported that *CDKAL1* variants decreased first-phase insulin secretion but not second-phase insulin in humans with type 2 diabetes. Thus, the altered expression of CDKAL1 is probably associated with reduced

glucose-induced first-phase insulin exocytosis and thus confers an increased risk for diabetes.

Although our data showed a critical role of CDKAL1 in insulin exocytosis *in vitro*, the *CDKAL1* KO mice had almost normal glucose homeostasis (N. Kato, in submission). The reason for the normal glucose homeostasis *in vivo*, despite reduced first-phase insulin release in vitro, is unknown, but there are several possibilities to be considered. First, the magnitude of the reduction in first-phase insulin release is not sufficient to cause impaired glucose tolerance in mice at this stage we examined. In fact, Stancakova et al. [11] reported that the SNP rs7754840 of *CDKAL1* is associated with impaired insulin secretion in non-diabetic offspring of type 2 diabetic subjects and in a large sample of men with normal glucose tolerance. Second, the role of CDKAL1 on the regulation of insulin exocytosis may have a limited influence on whole-body glucose metabolism. Therefore, additional genetic and environmental factors may be needed to cause impaired glucose tolerance.

In summary, we have provided the first report documenting a role of CDKAL1 in β cells. Our study using *CDKAL1* KO mice shows that CDKAL1 controls first-phase insulin exocytosis in β cells by facilitating ATP generation, glucose-induced K_{ATP} channel responsiveness and subsequent Ca^{2+} channel activity. Defects in this process caused by decreased CDKAL1 expression levels may confer an increased risk of diabetes.

Methods

Generation of *CDKAL1* KO mice

CDKAL1 KO mice were generated by the gene-trapping method [27–29] at TransGenic Inc. (Kobe, Japan) and thereafter established as an experimental model at the National Center for Global Health and Medicine. Male mice were used at the age of 10–14 weeks. Animal experiments were approved by the Animal Care and Use Committee of NCGM Research Institute (permit number: 22-TG-35) and the Kyorin University Animal Care Committee (permit number: 65-2).

Islets and pancreatic β cells

Pancreatic islets of Langerhans were isolated from male WT and *CDKAL1* KO mice by collagenase digestion, as previously described [30]. The isolated islets were then dispersed and cultured [30]. To label the insulin secretory granules, pancreatic β cells were infected with recombinant adenovirus Adex1CA insulin–GFP [30].

RT-PCR

Total RNA was extracted using an Illusta kit (GE healthcare, Piscataway, NJ, USA), and the full-length *CDKAL1* was amplified by RT-PCR using specific primers (forward primer: ctctcagttcg-gacagattcatctttcaagaggac; reverse primer: gctgtgatctggtctgaggtca-gatggc; product 2 kb). The PCR product was separated on agarose gels.

Immunoblotting

Proteins were extracted from mouse pancreatic islets and whole brain and immunoblotted [12,31]. We used antibodies targeting the following proteins: CDKAL1 (ab68045, Abcam, Cambridge, UK), p35 (C19, Santa Cruz, CA, USA), CDK5 (DC17, Santa Cruz), syntaxin 1A (a gift from Dr. T. Fujiwara, Kyorin University School of Medicine, Tokyo, Japan), SNAP25 (Wako Pure Chemical Industries Ltd., Osaka, Japan), VAMP2 (StressGen Biotechnologies Corp, Victoria, BC, Canada), Kir6.2 (Santa Cruz), SUR1 (Santa Cruz), MEK-1/2 (Cell Signaling Technology, Beverly, MA, USA), BIP/GPR78 (BD Transduction Laboratories, Lexington, KY, USA), Bcl-2 (BD Transduction Laboratories) and β-actin (Sigma-Aldrich, St. Louis, MO, USA).

Morphometric analysis of islets

To analyze islet size and β cell mass, paraffin-embedded pancreas sections (10 μm) were labeled with anti-insulin antibodies and detected by an avidin-biotin-peroxidase technique (Vector Laboratories, Burlingame, CA, USA). Sections were collected at 500 μm intervals from tissue blocks, and all islets in the sections were analyzed to determine islet area as a percentage of total pancreatic area. Images were acquired with an Olympus microscope IX70 equipped with a charge-coupled device camera, and analyzed with Metamorph software (Molecular Devices, Downingtown, PA, USA).

Electron microscopy

Electron microscopy was carried out using previously described methods [12]. Tissues were fixed in phosphate-buffered 2.5% glutaraldehyde (pH 7.4), postosmicated, dehydrated with graded alcohols, and embedded in Epon 812. After staining with uranyl acetate and lead citrate, ultra-thin sections were examined under a transmission electron microscope (TEM-1010C, JEOL, Akishima, Tokyo, Japan). In electron microscopy, granules at their shortest distance of <10 nm from the plasma membrane were defined as morphologically docked granules.

Insulin content

To measure insulin content in the whole pancreas, the excised pancreata were frozen in liquid nitrogen and disrupted with Cryopress (Microtech Nichion, Funabashi, Japan). The resulting powder was then suspended in cold acid-ethanol, and insulin was extracted overnight at 4°C [32]. The supernatants were diluted and subjected to enzyme-linked immunosorbent assays (ELISA) as described previously [12]. Insulin content per isolated islet was measured by ELISA [12]. Hoechst-33258 staining of sonicated islets was performed to determine the islet DNA content.

Insulin release in batch incubated β cells

Batch incubation experiments for insulin release have been described elsewhere [33]. Briefly, after plating WT and KO cells on 96-well plates, the cells were preincubated for 30 min in Krebs-Ringer buffer (KRB) containing (in mM): 110 NaCl, 4.4 KCl, 1.45 KH_2PO_4, 1.2 $MgSO_4$, 2.3 calcium gluconate, 4.8 $NaHCO_3$, 2.2 glucose, 10 HEPES, pH 7.4, and 0.3% bovine serum albumin (BSA), and then challenged with 2.2 mM glucose or 22 mM glucose for 30 min. At the end of the stimulation period, the cells were disrupted by sonication and aliquots of media and cell extracts were analyzed by ELISA. The released insulin is expressed as a percentage of total cellular content.

TIRF microscopy

The Olympus total internal reflection system with a high-aperture objective lens was used as described previously [12]. Briefly, primary β cells expressing insulin–GFP on the glass cover slip (Olympus, Tokyo, Japan) were mounted in an open chamber and incubated for 30 min with KRB. Cells were then transferred to a thermostat-controlled stage (37°C) and stimulated with 22 mM glucose (final) and 40 mM KCl (final). To evaluate the number of docked insulin granules by TIRF microscopy, wild-type and *CDKAL1* knockout cells were cultured on high refractive index glass, fixed, permeabilized with 4% paraformaldehyde/0.1% Triton X-100, and processed for immunohistochemistry [12].

Cells were labeled with anti-insulin antibodies (Sigma-Aldrich) and processed with goat anti-mouse IgG conjugated to Alexa Fluor-488 (Molecular probes, Eugene, OR, USA). Immunofluorescence was detected by TIRF microscopy.

Measurements of intracellular free Ca^{2+} ($[Ca^{2+}]_i$)

Fura-2 acetoxymethyl ester (Fura-2 AM: Molecular Probes) was loaded into cultured β cells and the ARGUS/HiSCA system (Hamamatsu photonics, Hamatsu, Japan) was used for measurement, as previously described [12].

Patch-clamp experiments in mouse single β cells

Perforated whole-cell currents were recorded using a pipette solution containing amphotericin B (200 μg/ml) dissolved in 0.1% DMSO [34]. Membrane currents were recorded using an amplifier (200B; Axopatch, Foster, CA) and stored online in a computer running pCLAMP10.2 software. The voltage clamp in perforated mode was considered to be adequate when the series resistance was <20 MΩ. Patch pipettes were pulled from glass tubes (Narishige, Tokyo, Japan); the resistances of the pipettes ranged from 4 to 7 MΩ when filled with the pipette solution containing 40 mM K_2SO_4, 50 mM KCl, 5 mM $MgCl_2$, 0.5 mM EGTA and 10 mM HEPES at pH 7.2 with KOH. To record the K_{ATP} channel current, the β cells were voltage-clamped to the holding potential of −70 mV, stepped to −100 mV to apply the voltage ramp from −100 to −50 mV at a speed of 5 mV/100 ms, and stepped back to −70 mV every 10 s. Electrophysiological experiments were performed at room temperature (25°C).

Measurement of islet ATP content

The ATP content of pancreatic islets was measured by HPLC using a modified version of previously described methods [35,36]. Experiments were performed on islets from WT and KO mice after incubation overnight in RPMI containing 11 mM glucose. Groups of 25 islets were hand-picked and preincubated in KRB containing 2.2 mM glucose for 60 min. After preincubation, the islets were incubated for 5 min in KRB containing 2.2 or 22 mM glucose. Then, ATP was extracted with 0.4 M perchloric acid and assayed by HPLC with a reversed-phase SUPELCOSIL column (LC-18-T, 3 μm, 15×4.6 mm, Sigma-Aldrich) according to the manufacturer's instructions. ATP levels were standardized to protein concentrations.

Mitochondrial membrane potential

WT and KO cells cultured on cover glass were loaded with 10 nM TMRE (Molecular Probes) [15] for 45 min in KRB containing 2.2 mM glucose and washed and incubated for a further 15 min with KRB. We obtained TMRE fluorescence images from multiple individual cells before and after increasing the extracellular glucose concentration from 2.2 mM to 22 mM or with 10 mM KIC (Nakarai Tesque Inc, Kyoto Japan) using confocal fluorescent microscopy (FV-1000, Olympus) [543-nm laser line and emission filter set (BA 560–620)].

Immunoprecipitation and detection of the histone H1 kinase activity of CDK5

The kinase activity of CDK5/p35 was measured after immunoprecipitation with anti-p35 antibody, as previously described [31]. Briefly, the isolated islets were sonicated in MOPS buffer (20 mM MOPS, pH 6.8, 1 mM EGTA, 0.1 mM EDTA, 0.3 M NaCl, 1 mM $MgCl_2$, 0.5% Nonidet P-40, 0.2 mM Pefabloc SC, 1 mg/ml leupeptin, and 1 mM DTT), and centrifuged at 20,000×g for 30 min to collect the supernatant. The kinase activity of CDK5-p35 immunoprecipitated with anti-p35 antibody (C19, Santa Cruz) from an equal protein amount of islet extract was measured using histone H1 as a substrate in the absence or presence of 20 μM roscovitine.

Subcellular localization of CDKAL1 in β cells

Fractionation by differential centrifugation was performed with minor modification as described previously [17]. MIN6 β cells (a gift from Dr. J.-I. Miyazaki, Osaka University, Osaka, Japan) were homogenized in sucrose buffer (5 mM HEPES (pH 7.5), 0.32 M sucrose, and protease inhibitors). The homogenates were centrifuged at 800×g for 10 min to obtain the postnuclear supernatant (S1). S1 was centrifuged at 8,900×g for 15 min to separate the S2 soluble cytosolic/microsomal fraction and precipitate. The precipitate was resuspended in sucrose buffer, and centrifuged at 540,000×g for 2 h, to yield the pellet (membrane fraction). The S2 fraction was centrifuged for 1 h at 540,000×g for 2 h, yielding a soluble cytosolic fraction (S3). Equal amounts (2 μg protein) of the fractions were separated by SDS-PAGE and immunoblotted with specific antibodies.

EGFP–CDKAL1 was generated using a cDNA fragment encoding a full open reading frame of murine CDKAL1 (Dnaform, Kanagawa, Japan), N-terminally tagged with EGFP, and subcloned into the HindIII/KpnI site of a pcDNA3 vector (Invitrogen). For immunohistochemical localization of CDKAL1, MIN6 β cells were transfected with EGFP–CDKAL1 using Lipofectamine2000 (Invitrogen) according to the manufacturer's instructions and cultured for 2 days. The intracellular localization was examined under a confocal microscope with MitoTracker (Red CM-H2XRos, Molecular probes) staining (100 nM for 20 min) or immunostaining (fixed and permeabilized with 4% paraformaldehyde/0.1% Triton X-100) with anti-calnexin antibody.

Author Contributions

Conceived and designed the experiments: MOI SN. Performed the experiments: MOI MY KA TS HT YA YN MK. Analyzed the data: CN HK SH. Contributed reagents/materials/analysis tools: TO RTY NK. Wrote the paper: MOI SN.

References

1. Zeggini E, Weedon MN, Lindgren CM, Frayling TM, Elliott KS, et al. (2007) Replication of genome-wide association signals in UK samples reveals risk loci for type 2 diabetes. Science 316: 1336–1341.
2. Steinthorsdottir V, Thorleifsson G, Reynisdottir I, Benediktsson R, Jonsdottir T, et al. (2007) A variant in CDKAL1 influences insulin response and risk of type 2 diabetes. Nature Genetics 39: 770–775.
3. Diabetes Genetics Initiative of Broad Institute of Harvard and MIT LU, and Novartis Institutes of BioMedical Research:, Saxena R, Voight BF, Lyssenko V, Burtt NP, de Bakker PI, et al. (2007) Genome-wide association analysis identifies loci for type 2 diabetes and triglyceride levels. Science 316: 1331–1336.
4. Scott LJ, Mohlke KL, Bonnycastle LL, Willer CJ, Li Y, et al. (2007) A genome-wide association study of type 2 diabetes in Finns detects multiple susceptibility variants. Science 316: 1341–1345.
5. Takeuchi F, Serizawa M, Yamamoto K, Fujisawa T, Nakashima E, et al. (2009) Confirmation of multiple risk Loci and genetic impacts by a genome-wide association study of type 2 diabetes in the Japanese population. Diabetes 58: 1690–1699.
6. Ching YP, Pang AS, Lam WH, Qi RZ, Wang JH (2002) Identification of a neuronal Cdk5 activator-binding protein as Cdk5 inhibitor. J Biol Chem 277: 15237–15240.
7. Ubeda M, Kemp DM, Habener JF (2004) Glucose-induced expression of the cyclin-dependent protein kinase 5 activator p35 involved in Alzheimer's disease regulates insulin gene transcription in pancreatic beta-cells. Endocrinology 145: 3023–3031.
8. Wei FY, Nagashima K, Ohshima T, Saheki Y, Lu YF, et al. (2005) Cdk5-dependent regulation of glucose-stimulated insulin secretion. Nat Med 11: 1104–1108.

9. Ubeda M, Rukstalis JM, Habener JF (2006) Inhibition of cyclin-dependent kinase 5 activity protects pancreatic beta cells from glucotoxicity. J Biol Chem 281: 28858–28864.
10. Groenewoud MJ, Dekker JM, Fritsche A, Reiling E, Nijpels G, et al. (2008) Variants of CDKAL1 and IGF2BP2 affect first-phase insulin secretion during hyperglycaemic clamps. Diabetologia 51: 1659–1663.
11. Stancakova A, Pihlajamaki J, Kuusisto J, Stefan N, Fritsche A, et al. (2008) Single-nucleotide polymorphism rs7754840 of CDKAL1 is associated with impaired insulin secretion in nondiabetic offspring of type 2 diabetic subjects and in a large sample of men with normal glucose tolerance. J Clin Endocrinol Metab 93: 1924–1930.
12. Ohara-Imaizumi M, Fujiwara T, Nakamichi Y, Okamura T, Akimoto Y, et al. (2007) Imaging analysis reveals mechanistic differences between first- and second-phase insulin exocytosis. J Cell Biol 177: 695–705.
13. Cook DL, Hales CN (1984) Intracellular ATP directly blocks K+ channels in pancreatic B-cells. Nature 311: 271–273.
14. Ohno-Shosaku T, Zunkler BJ, Trube G (1987) Dual effects of ATP on K+ currents of mouse pancreatic beta-cells. Pflugers Arch 408: 133–138.
15. Heart E, Corkey RF, Wikstrom JD, Shirihai OS, Corkey BE (2006) Glucose-dependent increase in mitochondrial membrane potential, but not cytoplasmic calcium, correlates with insulin secretion in single islet cells. Am J Physiol Endocrinol Metab 290: E143–E148.
16. Duchen MR, Smith PA, Ashcroft FM (1993) Substrate-dependent changes in mitochondrial function, intracellular free calcium concentration and membrane channels in pancreatic beta-cells. Biochem J 294(Pt 1): 35–42.
17. Hosokawa T, Saito T, Asada A, Ohshima T, Itakura M, et al. (2006) Enhanced activation of Ca2+/calmodulin-dependent protein kinase II upon downregulation of cyclin-dependent kinase 5-p35. J Neurosci Res 84: 747–754.
18. Giroix MH, Sener A, Bailbe D, Leclercq-Meyer V, Portha B, et al. (1993) Metabolic, ionic, and secretory response to D-glucose in islets from rats with acquired or inherited non-insulin-dependent diabetes. Biochem Med Metab Biol 50: 301–321.
19. Portha B, Lacraz G, Kergoat M, Homo-Delarche F, Giroix MH, et al. (2009) The GK rat beta-cell: a prototype for the diseased human beta-cell in type 2 diabetes? Mol Cell Endocrinol 297: 73–85.
20. Chen L, Koh DS, Hille B (2003) Dynamics of calcium clearance in mouse pancreatic beta-cells. Diabetes 52: 1723–1731.
21. Hughes E, Lee AK, Tse A (2006) Dominant role of sarcoendoplasmic reticulum Ca^{2+}-ATPase pump in Ca^{2+} homeostasis and exocytosis in rat pancreatic beta-cells. Endocrinology 147: 1396–1407.
22. Walter L, Hajnoczky G (2005) Mitochondria and endoplasmic reticulum: the lethal interorganelle cross-talk. J Bioenerg Biomembr 37: 191–206.
23. Schroder M, Kaufman RJ (2005) ER stress and the unfolded protein response. Mutat Res 569: 29–63.
24. Eizirik DL, Cardozo AK, Cnop M (2008) The role for endoplasmic reticulum stress in diabetes mellitus. Endocr Rev 29: 42–61.
25. Lei X, Zhang S, Bohrer A, Ramanadham S (2008) Calcium-independent phospholipase A2 (iPLA2 beta)-mediated ceramide generation plays a key role in the cross-talk between the endoplasmic reticulum (ER) and mitochondria during ER stress-induced insulin-secreting cell apoptosis. J Biol Chem 283: 34819–34832.
26. Arragain S, Handelman SK, Forouhar F, Wei FY, Tomizawa K, et al. (2010) Identification of eukaryotic and prokaryotic methythiotransferases for biosynthesis of 2-methylthio-N6-threonylcarbamoyladenosine in tRNA. J Biol Chem 285: 28425–28433.
27. Araki K, Imaizumi T, Sekimoto T, Yoshinobu K, Yoshimuta J, et al. (1999) Exchangeable gene trap using the Cre/mutated lox system. Cell Mol Biol (Noisy-le-grand) 45: 737–750.
28. Taniwaki T, Haruna K, Nakamura H, Sekimoto T, Oike Y, et al. (2005) Characterization of an exchangeable gene trap using pU-17 carrying a stop codon-beta geo cassette. Dev Growth Differ 47: 163–172.
29. Yagi T, Tokunaga T, Furuta Y, Nada S, Yoshida M, et al. (1993) A novel ES cell line, TT2, with high germline-differentiating potency. Anal Biochem 214: 70–76.
30. Ohara-Imaizumi M, Nishiwaki C, Kikuta T, Nagai S, Nakamichi Y, et al. (2004) TIRF imaging of docking and fusion of single insulin granule motion in primary rat pancreatic beta-cells: different behaviour of granule motion between normal and Goto-Kakizaki diabetic rat beta-cells. Biochem J 381: 13–18.
31. Saito T, Onuki R, Fujita Y, Kusakawa G, Ishiguro K, et al. (2003) Developmental regulation of the proteolysis of the p35 cyclin-dependent kinase 5 activator by phosphorylation. J Neurosci 23: 1189–1197.
32. Filipponi P, Marcelli M, Nicoletti I, Pacifici R, Santeusanio F, et al. (1983) Suppressive effect of long term sulfonylurea treatment on A, B, and D cells of normal rat pancreas. Endocrinology 113: 1972–1979.
33. Ohara-Imaizumi M, Nakamichi Y, Tanaka T, Ishida H, Nagamatsu S (2002) Imaging exocytosis of single insulin secretory granules with evanescent wave microscopy: distinct behavior of granule motion in biphasic insulin release. J Biol Chem 277: 3805–3808.
34. Nakazaki M, Kakei M, Ishihara H, Koriyama N, Hashiguchi H, et al. (2002) Association of upregulated activity of K(ATP) channels with impaired insulin secretion in UCP1-expressing insulinoma cells. J Physiol 540: 781–789.
35. Komatsu M, Noda M, Sharp GW (1998) Nutrient augmentation of Ca2+-dependent and Ca2+-independent pathways in stimulus-coupling to insulin secretion can be distinguished by their guanosine triphosphate requirements: studies on rat pancreatic islets. Endocrinology 139: 1172–1183.
36. Dukes ID, Sreenan S, Roe MW, Levisetti M, Zhou YP, et al. (1998) Defective pancreatic beta-cell glycolytic signaling in hepatocyte nuclear factor-1alpha-deficient mice. J Biol Chem 273: 24457–24464.

World J Surg (2011) 35:512–519
DOI 10.1007/s00268-010-0865-x

World Journal of Surgery

Simplified Alternative to the TRISS Method for Resource-Constrained Settings

Shinji Nakahara · Masao Ichikawa · Akio Kimura

Published online: 19 November 2010

Abstract
Background We developed simple methods of risk adjustment for evaluating the quality of injury care (predicting survival probabilities of the injured) by fully utilizing routinely collected data in injury surveillance and clinical practices. Widely used methods of risk adjustment require additional data that are difficult to collect in resource-constrained settings.
Methods We developed logistic regression models that predict survival using data obtained from 9,840 victims aged 15 years or older with blunt traumatic injuries who were registered in the Japan Trauma Data Bank, Japan's national trauma registry, between January 2004 and December 2007. The models included three predictors: age, an anatomical injury severity parameter such as a simplified severity categorization (minor, moderate, and severe) described in the *Injury Surveillance Guidelines*, and a physiological status parameter. The models' abilities to predict survival probabilities were evaluated using the area under the receiver-operating characteristic curve (AUROCC).
Results The simplified three-predictor models showed good performance with the AUROCC ranging from 0.86 to 0.94. In particular, the models with a consciousness level indicator as a physiological parameter showed a high AUROCC, ranging from 0.93 to 0.94, which was not much different from the performance of the widely used method that shows an AUROCC of 0.96.
Conclusions Simplified methods of risk adjustment that require only routinely collected data will facilitate evaluation and improvement in the quality of injury care in resource-constrained low- and middle-income countries, where injuries are a growing public health concern.

Introduction

Injuries are a growing public health concern, killing more than 5 million people every year worldwide; more than 90% of injury deaths occur in low- and middle-income countries (LMICs) [1]. Prevention of injury deaths requires improvement in the care of the injured, as well as implementation of injury prevention measures. Quality improvement of injury treatment, including a prehospital emergency care system, is an important component in strengthening health care systems in LMICs with limited human and physical resources for injury care, as has been shown by studies based on the Guidelines for Essential Trauma Care [2–5].

Quality of care comprises three elements: structure (resources and capacities), process (how patients are treated), and outcome (survival, adverse events, or subsequent disabilities) [4]. Improvements in structure and process are intermediate steps in the pursuit of outcome improvement;

A part of this study was presented at the 24th annual conference of the Japan Association for the Surgery of Trauma, in Chiba, Japan, held May 27–28, 2010.

S. Nakahara (✉)
Department of Preventive Medicine, St. Marianna University School of Medicine, 2-16-1 Sugao, Miyamae-ku, Kawasaki, Kanagawa 216-8511, Japan
e-mail: snakahara@marianna-u.ac.jp

M. Ichikawa
Graduate School of Comprehensive Human Sciences, University of Tsukuba, Tsukuba, Ibaraki, Japan

A. Kimura
Department of Emergency Medicine, National Center for Global Health and Medicine Hospital, Tokyo, Japan

thus, outcome evaluation is a direct measurement of quality improvement. Objective comparison of injury outcomes between individuals or between hospitals requires methods of risk adjustment to control for case-mix severity.

Various risk adjustment methods have been developed: some based on the Abbreviated Injury Scale (AIS), some on physiological parameters alone, and some on the International Classification of Diseases (ICD) (Table 1) [4–7]. The AIS severity scores rate the severity of each of the sustained injuries from 1 (minor) to 6 (fatal). The Injury Severity Score (ISS) consists of the AIS severity scores for the three most severely injured body regions. The Revised Trauma Score (RTS) is a physiological score consisting of the Glasgow Coma Scale (GCS) score indicating consciousness level using three components (motor, verbal, and eye opening), respiratory rate (RR), and systolic blood pressure (SBP). The Trauma and Injury Severity Score (TRISS) is a logistic regression model that predicts survival probabilities (Ps), and comprises the ISS and RTS, age, and injury mechanisms. There is also a method based on the ICD codes, named the ICD-based Injury Severity Score (ICISS), in which the survival risk ratio (SRR) for each code is empirically derived from the data [8].

These methods seem inappropriate in resource-constrained settings owing to difficulties in collecting information. For example, TRISS is a complicated composite of several parameters including AIS severity scores and GCS scores, which may not be routinely collected. Because accurate use of the AIS and GCS requires appropriate training, collecting such information poses challenges to LMICs with additional cost [9]. Furthermore, the more parameters are required, the more frequently missing data occur. The ICISS does not require additional use of the AIS to describe injury severity; however, it does require large data sets to calculate the SRRs for each injury code, including rare ones, which is also a challenging task for LMICs, particularly those with small populations [10].

Alternative simple methods have also been developed. The Kampala Trauma Score (KTS) developed in Uganda is an example of a simplified TRISS-like scale, in which the ISS and GCS scores are replaced by the number of serious injuries with three categories and the four-point consciousness scale, respectively (Table 1) [11]. Attempts to simplify the TRISS in high-income countries (HICs) include replacing the multiple-injury scores (ISS) with the worst injury score alone, replacing the total GCS scores

Table 1 Risk adjustment methods

GlasgowComaScale(GCS) = GCSm + GCSv + GCSe

GCSm = motor component indicating best motor response, ranging from 1 (no response) to 6 (moves limb to command)

GCSv = verbal component indicating best verbal response, ranging from 1 (no response) to 5 (oriented response)

GCSe = eye component indicating eye opening response, ranging from 1 (no response) to 4 (opens spontaneously)

RevisedTraumaScore(RTS) = $0.9364 \times \text{GCS} + 0.7326 \times \text{SBP} + 0.2908 \times \text{RR}$[a]

The coefficients were derived from the Major Trauma Outcome Study (MTOS)

Injury Severity Score(ISS) = $\text{AIS}_1^2 + \text{AIS}_2^2 + \text{AIS}_3^2$

The ISS is the sum of three squared AIS severity scores in the three most severely injured anatomical body regions (out of 6 regions); 1 AIS score is derived from a single region

Trauma and Injury Severity Score (TRISS)

Logit(Ps) = $\alpha + \beta_1 \times \text{RTS} + \beta_2 \times \text{ISS} + \beta_3 \times \text{Age}$[a]

Coefficients derived from the MTOS are:

	Constant (α)	RTS (β_1)	ISS (β_2)	Age (β_3)
Blunt	−0.4499	0.8085	−0.0835	−1.7430
Penetrating	−2.5355	0.9934	−0.0651	−1.1360

ICD-based Injury Severity Score(ICISS) = $\text{SRR}_{\text{inj1}} \times \text{SRR}_{\text{inj2}} \times \text{SRR}_{\text{inj3}} \times \cdots \times \text{SRR}_{\text{injn}}$

The Survival Risk Ratio (SRR) for each code is empirically derived from the data: the number of patients who survived with a certain ICD code divided by the total number of patients with injuries. The ICISS is the product of all the SRRs in a patient: from SRR_{inj1} (SRR for injury 1) to SRR_{injn} (SRR for injury n)

Kampala Trauma Score(KTS) = Age + SBP + RR + AVPU + No. of serious injuries[a]

All parameters are coded: age is coded as in the TRISS; codes used in the RTS (5 points) are collapsed for SBP (4 points) and RR (3 points); The number of injuries is coded into 3 categories (nil, single, or multiple)

Source: Refs. [4, 6, 7, 11]

SBP systolic blood pressure, *RR* respiratory rate, *AIS* abbreviated injury scale, *AVPU scale* four-point consciousness scale (alert, responsive to verbal stimuli, responsive to painful stimuli, and unconscious)

[a] Age, GCS, SBP, and RR are coded

with the GCS motor component (GCSm), and developing a model with only the three parameters of age, worst injury SRR, and GCSm [12–14]. These methods perform quite well, even better than the TRISS; however, they have not fully addressed the issue of difficulties in collecting necessary information. The KTS requires five parameters, and the number of serious injuries included in the parameters may not be available in other countries; the simplified version of TRISS in HICs requires AIS severity scores, ICISS-based SRRs, or GCS scores.

Given the reality of the situations faced in LMICs, we need simplified methods based only on readily obtainable information. A study in Canada indicated that inclusion of age and a physiological parameter in the predictive models would minimize differences in the predictive ability of anatomical injury severity indicators, posing the possibility that models including the three parameters would show similar performance regardless of the types of indicators used [15]. In countries where injury surveillance has begun based on the *Injury Surveillance Guidelines* prepared by the World Health Organization, a simplified global severity indicator (minor, moderate, or severe) described in the guidelines is available [16, 17]. Simple physiological indicators can be obtained from clinical records. Therefore, we developed methods with a minimum set of parameters using easily obtainable indicators.

Methods

Study design, population, and settings

We developed logistic regression models that predict the survival probabilities of injured victims on the basis of three simplified predictors—age, anatomical injury severity, and physiological status—using data derived from the Japan Trauma Data Bank (JTDB). The JTDB is Japan's national trauma registry. Participating facilities are critical care medical centers and emergency departments of tertiary care hospitals, which are equivalent to level 1 trauma centers; hospitalized patients in the participating facilities are registered [17, 18]. Because participation in the JTDB is voluntary, some facilities are participating but others are not, depending on their resource availabilities and wishes [19]. Data included in the JTDB are age, sex, injury mechanisms, type of injury (penetrating, blunt, burn, or other), physiological status at the scene and at-hospital arrival, AIS codes including severity score for all injuries, prehospital care, survival, length of ICU and hospital stay, and treatment details [17].

Study participants were patients 15 years of age or older with blunt traumatic injuries who were hospitalized and registered in the JTDB between January 2004 and December 2007. Of the eligible 16,716 participants, 12,437 had information on age, AIS severity scores, and physiological status on arrival (GCS, SBP, and RR), which are necessary to calculate TRISS-based Ps; 9,840 had outcome information (survived or not) and thus were included in the model development. We did not model the Ps of penetrating and pediatric injuries owing to the insufficient number of victims in the database. The protocol of the present study was approved by the ethics committee of St. Marianna University School of Medicine.

Models and parameters

The models developed in this study are described as:

$$\text{Logit(Ps)} = \beta_0 + \beta_1 \times \text{age} + \beta_2 \times \text{severity} + \beta_3 \times \text{physiology},$$

where β_x denotes a regression coefficient; β_0 denotes the intercept point; β_{1-3} denote coefficients for the three predictors; age indicates age; severity indicates anatomical injury severity (worst injury AIS severity scores [maxAIS], collapsed AIS severity categories, or number of serious injuries); and physiology indicates physiological status (GCS, GCSm, AVPU [four-point consciousness scale], SBP, or RR). Each model includes each of these injury severity and physiological status indicators as predictors; widely used indicators (maxAIS and GCS) were also included so that we could compare their predictive abilities with those of the simplified indicators. All indicators other than those for the maxAIS and GCSm were categorized and coded, as shown in Table 2. The coded values of age, GCS score, SBP, and RR are the same as those used in the TRISS and RTS. The coded values of the number of serious injuries are the same as those of the KTS. To compare the performance of the three-predictor models with the widely used TRISS method, the JTDB-derived TRISS model was fitted.

The maxAIS, a six-point scale, was collapsed into three categories in three ways to simulate possible variations in the usage of the simplified global injury severity categories of "minor," "moderate," and "severe" described in the *Injury Surveillance Guidelines* [16], assuming that the global severity can be judged on the basis of the severest injury (Table 2). We defined serious injuries as those with AIS severity scores of 3 or more for the number of serious injuries. The 12-point GCS score was collapsed into four categories to simulate the usage of the four-point AVPU (Alert, responsive to Verbal stimuli, responsive to Painful stimuli, and Unconscious) scale according to the report by Kobusingye and Lett that showed that the AVPU corresponded well to GCS scores [11].

Because variations or misclassifications are likely to occur in the actual classification practices using the

Table 2 Coded values of categorized indicators

Coded value	GCS score	SBP (mmHg)	RR (/min)	Age	AVPU	Collapsed Max AIS (a)	Collapsed Max AIS (b)	Collapsed Max AIS (c)	No. of serious injuries
4	13–15	>89	10–29						
3	9–12	76–89	>29		GCS 14–15				
2	6–8	50–75	6–9		GCS 11–13	AIS 1–2	AIS 1–2	AIS 1	2+
1	4–5	1–49	1–5	55+	GCS 5–10	AIS 3–4	AIS 3	AIS 2	1
0	3	0	0	0–54	GCS 3–4	AIS 5–6	AIS 4–6	AIS 3–6	0

simplified categorizations (global severity categories and the AVPU scale), simulating the use of these simplified categories just by collapsing the AIS severity scores and GCS scores is unrealistic. Therefore, we developed a model that includes as predictors a mixture of the three ways of collapsing the AIS severity scores and a mixture of the two different ways of collapsing the GCS scores to simulate the variations. For each participant, one of the three ways of collapsing the AIS and one of the two ways of collapsing the GCS scores (i.e., the AVPU scale or the GCS scores 3–5, 6–9, 10–12, and 13–15 coded from 0 to 3) were randomly selected to make mixed indicators.

Analyses

We obtained estimates for the models' regression coefficients using the maximum likelihood estimation with survival being the outcome (survival = 1; nonsurvival = 0). A 10-fold cross-validation was used to compute the predicted Ps from the model estimates. The data were randomly divided into 10 subgroups; 9 subgroups (training data sets) were used to estimate the coefficients, which were applied to the remaining subgroup (validation data set) to obtain the predicted Ps, in a round of cross-validation. This process was repeated an additional nine times. We recorded the averages of the 10 sets of coefficients. The predicted probability values were used to evaluate the models' ability to distinguish survivors from nonsurvivors and the models' goodness-of-fit (calibration). The area under the receiver-operating characteristics curve (AUROCC), which ranges from 0.5 to 1, was calculated to evaluate the discrimination ability (values nearer to 1 indicate better abilities). The Hosmer–Lemeshow (H–L) statistic was used to evaluate the calibration. The H–L statistic indicates the degree of difference between the predicted and observed numbers of survivors in each decile of predicted Ps (smaller H–L values indicate better calibration) [20]. Because of the very large sample size, we used neither statistical tests with obviously small p values nor narrow confidence intervals. Model fitting was done with SPSS version 17. To indicate how the simplified models can be easily used even without a calculator, we developed lookup tables showing Ps for each set of predictive variables (see Appendices A and B).

Results

Table 3 shows the characteristics of the study population. The majority of the 9,840 analyzed participants were male, younger than 55 years of age, and with sustained unintentional injuries due to traffic crashes or falls; 18% of them died after admission. Those with injuries of minor to moderate severity (ISS < 15) accounted for about half the study population. Most of the participants showed normal physiological status on hospital arrival.

Table 4 shows the coefficients of the tested models (averaged values from the 10-fold cross-validation), AUROCC, and H–L statistic. The TRISS model showed the best AUROCC. Among the three-predictor models, those with maxAIS and GCS scores showed a marginally better AUROCC (0.949) than did the others. Among the models with collapsed AIS severity categories or number of serious injuries, those with the GCSm or AVPU as the physiological parameter showed quite good performance, with an AUROCC ranging from 0.930 to 0.944, whereas those with BP or RR as the physiological parameter showed a lower AUROCC, ranging from 0.861 to 0.93 1. Models with the GCSm or AVPU did not differ in AUROCC; in the majority of models, those with the AVPU showed lower H–L values than did those with the GCSm. The model including mixed indicators as explained in the "Models and parameter" had an AUROCC of 0.935 and an H–L value of 51.5 (not shown in Table 4). Appendices A and B show examples of lookup tables for two models.

Discussion

The present study showed that the models using easily obtainable simple indicators showed fairly good performance in predicting Ps of blunt traumatic injuries as long as they included the three parameters of age, anatomical injury severity, and physiological status. As a physiological

Table 3 Characteristics of the eligible and analyzed participants

	Eligible (n = 16,716)		Analyzed (n = 9,840)	
	n	%	n	%
Age (years)				
15–54	8,861	53.0	5,471	55.6
55+	7,855	47.0	4,369	44.4
Sex				
F	5,312	31.8	3,003	30.5
M	11,402	68.2	6,835	69.5
Missing	2		2	
Survival				
Died	2,101	17.6	1,769	18.0
Survived	9,816	82.4	8,071	82.0
Missing	4,799		0	
Intention (cause)				
Unintentional	14,924	91.4	8,723	90.7
Self harm	1,086	6.6	695	7.2
Violence	259	1.6	170	1.8
Other	63	0.4	34	0.4
Missing	384		218	
Mechanism				
Traffic	8,766	54.2	5,454	56.7
Fall	5,956	36.8	3,344	34.8
Other	1,447	8.9	814	8.5
Missing	547		228	
Injury Severity Score				
1–8	3,018	20.4	1,790	18.2
9–14	4,723	32.0	3,051	31.0
15–25	4,035	27.3	2,822	28.7
26–45	2,427	16.4	1,731	17.6
46–75	572	3.9	446	4.5
Missing	1,941		0	
Systolic blood pressure (mmHg)				
90+	13,071	85.5	8,275	84.1
76–89	495	3.2	325	3.3
50–75	398	2.6	254	2.6
1–49	195	1.3	129	1.3
0	1,125	7.4	857	8.7
Missing	1,432		0	
Respiratory rate (min)				
10–29	10,670	77.1	7,542	76.6
30+	1,925	13.9	1,348	13.7
6–9	60	0.4	41	0.4
1–5	19	0.1	16	0.2
0	1,172	8.5	893	9.1
Missing	2,870		0	
Glasgow Coma Scale				
13–15	12,832	76.8	7,078	71.9
9–12	1,018	6.1	684	7.0
6–8	822	4.9	581	5.9
4–5	373	2.2	261	2.7
3	1,671	10.0	1,236	12.6
Time to emergency room (min)				
<30	4,343	34.1	2,974	33.7
30–59	6,868	53.9	4,793	54.4
60–89	998	7.8	693	7.9
90–119	230	1.8	151	1.7
120+	311	2.4	206	2.3
Missing	3,966		1,023	

indicator, the AVPU may be the potential candidate for actual use because it showed better discrimination ability than did SBP or RR and better calibration than did the GCSm; any type of simplified anatomical injury severity indicator showed similar abilities. These findings suggest that we can further simplify the previously developed simplified models by reducing the number of variables and replacing complicated variables with simple ones.

In under-resourced settings in LMICs, particularly in rural areas, the limited resources allow neither two separate data collection systems for two different purposes, one for injury prevention and the other for quality improvement, nor collection of additional information such as the AIS and GCS. Considerable additional cost is required to establish two systems and introduce the AIS and GCS, which require costly training, to countries where such indicators are not now in use.

Using the simplified models developed in the present study would enable the use of injury surveillance data for both injury prevention and risk adjustment in quality evaluation without significant additional cost. Many LMICs are establishing or have already established injury surveillance systems on the basis of the *Injury Surveillance Guidelines,* which are likely to include the simple global severity categorization (minor, moderate, or severe) [16, 17]. Physiological indicators routinely collected in clinical practice can be easily added to the injury surveillance. Our findings suggest that level of consciousness has better performance than hemodynamic or respiratory status. Thus, the GCS or AVPU scale should be used whenever possible as the physiological indicator in the models, and SBP or RR should be used as the second option if the consciousness level indicator is not available.

An advantage of parsimonious models with fewer parameters is that limited combinations of the parameter codes result in a limited number of Ps. This would enable the use of simple lookup tables like those shown in Appendices A and B. Survival probabilities can be obtained

Table 4 Model coefficients, discrimination abilities, and calibrations

Models	Estimates for regression coefficients				AUROCC	H–L
	Constant	Age	Anatomical Injury Severity	Physiological status		
TRISS (age, ISS, RTS)	−1.82	−1.32	−0.07	0.94	0.962	61.2
Age, MaxAIS, GCS	2.32	−0.90	−0.87	1.17	0.949	37.2
Age, MaxAIS, GCSm	1.86	−0.86	−0.98	0.89	0.947	48.6
Age, MaxAIS, SBP	3.39	−0.89	−1.49	1.35	0.941	25.7
Age, MaxAIS, RR	3.19	−0.98	−1.50	1.43	0.934	7.0
Age, cMaxAIS(a), GCSm	−3.16	−0.88	1.54	0.91	0.943	45.3
Age, cMaxAIS(a), AVPU	−1.59	−0.83	1.20	1.58	0.944	32.4
Age, cMaxAIS(a), SBP	−4.22	−0.91	2.37	1.37	0.931	14.4
Age, cMaxAIS(a), RR	−4.42	−1.00	2.35	1.44	0.924	14.2
Age, cMaxAIS(b), GCSm	−2.81	−0.83	1.43	0.94	0.943	28.1
Age, cMaxAIS(b), AVPU	−1.28	−0.78	1.12	1.63	0.942	32.4
Age, cMaxAIS(b), SBP	−3.33	−0.79	1.97	1.35	0.920	42.7
Age, cMaxAIS(b), RR	−3.62	−0.88	2.03	1.44	0.913	22.7
Age, cMaxAIS(c), GCSm	−2.66	−0.84	2.48	1.00	0.930	64.7
Age, cMaxAIS(c), AVPU	−1.14	−0.79	2.16	1.73	0.934	29.7
Age, cMaxAIS(c), SBP	−2.82	−0.79	2.77	1.38	0.869	29.7
Age, cMaxAIS(c), RR	−3.05	−0.87	2.92	1.46	0.861	32.6
Age, No of injuries, GCSm	−0.56	−1.03	−1.30	0.97	0.936	64.4
Age, No of injuries, AVPU	0.64	−0.96	−1.12	1.68	0.941	36.0
Age, No of injuries, SBP	−0.68	−0.97	−1.23	1.29	0.888	55.6
Age, No of injuries, RR	−0.69	−1.08	−1.40	1.38	0.884	56.5

AUROCC area under receiver-operating characteristic curve, *H–L* Hosmer–Lemeshow statistic, *ISS* injury severity score, *RTS* revised trauma score, *MaxAIS* worst injury AIS severity score, *GCS* Glasgow Coma Scale score, *GCSm* GCS motor component, *cMaxAIS* collapsed MaxAIS into three categories, *AVPU* four-point consciousness scale (alert, responsive to verbal stimuli, responsive to painful stimuli, and unconscious)

Age, GCS, cMaxAIS(a–c), SBP, RR, and AVPU were coded as shown in Table 2

quickly from such tables. However, if many parameters are used, the lookup tables will become large and complicated; thus, software to calculate the Ps may be required.

Furthermore, using fewer parameters can reduce the magnitude of the problems associated with missing data [21]. Scales like TRISS that require many parameters suffer from frequency of missing data. In the present study, 26% of the eligible participants were missing some of the information necessary to calculate TRISS-Ps. Even in HICs, it is not infrequent to find data missing in a trauma registry or in patient records in a tertiary care hospital [22, 23].

Some limitations of the present study should be noted. We used simulated simplified indicators to test the models instead of data actually collected on simple global injury severity, number of serious injuries, or the AVPU scale, because these were not available in the JTDB data. The good performance of the tested models might have resulted from the fact that the simulated indicators were derived by collapsing the AIS severity scores and GCS scores. This possibility, however, is unlikely. The different ways of collapsing the AIS severity scores yielded similar results; simulated variations or misclassifications in the actual utilization of the simplified indicators by mixing different ways of collapsing the AIS severity scores and the GCS scores also made marginal differences.

Another limitation is the lack of representativeness in the data in two ways. First, owing to missing data, only 59% of the eligible cases were analyzed. The differences in characteristics between the total eligible participants and the analyzed participants were small. (We did not perform statistical testing because the large sample size would make very small differences statistically significant.) Second, because participating in the JTDB is voluntary, the registered data might have overrepresented well-staffed facilities that are likely to participate [19]. Quality of care might be different between well-staffed and understaffed facilities.

Although we showed the potential usefulness of the simplified models, it should be noted that we should validate them with data actually collected in LMICs and, even more important, further studies should estimate the coefficients of the models for each country [24, 25]. The coefficients estimated in the present study based on

Japanese data may not apply to other countries with different situations (e.g., emergency care and transportation systems). Therefore, the lookup tables shown in Appendices A and B should be considered as a reference, and the development of country-specific tables is recommended.

Furthermore, given the different country-specific situations such as extremely long transportation time in LMICs (up to several hours in remote areas) [26], model modification may be necessary. In the present study, we did not include such factors because our primary purpose was to simplify the standard methods, which do not include a time factor (the relative contribution of a time factor to outcome prediction is small when using data collected in HICs) [27]. In addition, extrapolation of modeling based on short transportation time to situations with longer transportation times is inappropriate. Such model modification, if necessary, should be based on the data obtained in LMICs.

Finally, we could not test the models for pediatric and penetrating injuries owing to the insufficient number of such injuries in the JTDB. As the TRISS method shows, however, the same model (combination of parameters) may apply to both blunt and penetrating injuries, or to both adult and pediatric injuries, with different coefficients [28]. Further studies are also needed to validate the models and estimate coefficients for pediatric and penetrating injuries.

Conclusions

We developed simple models to predict survival probability for the purpose of risk adjustment in care quality evaluation with a performance level that is not very inferior to widely used models such as TRISS or models with worst injury severities. Our models do not require AIS severity scores or GCS scores, which are difficult to collect in resource-constrained settings. Although validation of the models from data actually collected in LMICs is needed, the findings open up the possibility of existing or emerging injury surveillance systems, which are designed for injury prevention, being also used for quality improvement activities.

Acknowledgments This work was supported by a Grant for Research on Global Health Issues from the Ministry of Health, Labour, and Welfare of Japan. The authors are grateful to F. Miyamasu (Medical English Communications Center of the University of Tsukuba) for grammatical revision of the text.

Conflict of interest none

Appendix

See Tables 5 and 6.

Table 5 Probability of survival chart by age, injury severity, and AVPU

	AVPU			
	A	V	P	U
Age ≥ 55 years				
Severity (cMaxAIS[c])				
Minor (MaxAIS = 1)	0.999	0.997	0.984	0.916
Moderate (MaxAIS = 2)	0.996	0.976	0.876	0.556
Severe (MaxAIS = 3–6)	0.963	0.823	0.451	0.127
Age < 55 years				
Severity (cMaxAIS[c])				
Minor (MaxAIS = 1)	1.000	0.999	0.993	0.960
Moderate (MaxAIS = 2)	0.998	0.989	0.940	0.734
Severe (MaxAIS = 3–6)	0.983	0.911	0.644	0.242

Model: Logit (Ps) = −1.14 − 0.79 × age + 2.16 × severity + 1.73 × AVPU

Table 6 Probability of survival chart by age, number of severe injuries, and AVPU

	AVPU			
	A	V	P	U
Age≥ 55 years				
No. of severe injuries				
0	0.991	0.954	0.794	0.420
1	0.973	0.871	0.559	0.192
2+	0.922	0.689	0.293	0.072
Age < 55 years				
No. of severe injuries				
0	0.997	0.982	0.910	0.655
1	0.990	0.947	0.768	0.383
2+	0.969	0.853	0.521	0.169

Model: Logit (Ps) = 0.64 − 0.96 × age − 1.12 × no. of injury + 1.68 × AVPU

References

1. WHO. Disease and injury regional estimates for 2004. Available at: http://www.who.int/healthinfo/global_burden_disease/estimates_regional/en/index.html. Accessed 15 September 2010
2. Mock C, Lormand JD, Goosen J et al. (2004) Guidelines for Essential Trauma Care, World Health Organization, Geneva
3. Mock C, Nguyen S, Quansah R et al (2006) Evaluation of trauma care capabilities in four countries using the WHO-IATSIC Guidelines for Essential Trauma Care. World J Surg 30:946–956
4. Mock C, Juillard C, Brundage S et al (eds) (2009) Guidelines for Trauma Quality Improvement Programmes. World Health Organization, Geneva
5. Nakahara S, Saint S, Sann S et al (2009) Evaluation of trauma care resources in health centers and referral hospitals in Cambodia. World J Surg 33:874–885

6. Champion HR (2002) Trauma scoring. Scand J Surg 91:12–22
7. Senkowski CK, McKenney MG (1999) Trauma scoring systems: a review. J Am Coll Surg 189:491–503
8. Osler T, Rutledge R, Deis J et al (1996) ICISS: an international classification of disease-9 based injury severity score. J Trauma 41:380–386
9. Kim Y, Jung KY, Kim CY et al (2000) Validation of the International Classification of Diseases 10th Edition-based Injury Severity Score (ICISS). J Trauma 48:280–285
10. Cryer C (2006) Severity of injury measures and descriptive epidemiology. Inj Prev 12:67–68
11. Kobusingye OC, Lett RR (2000) Hospital-based trauma registries in Uganda. J Trauma 48:498–502
12. Healey C, Osler TM, Rogers FB et al (2003) Improving the Glasgow Coma Scale score: motor score alone is a better predictor. J Trauma 54:671–678
13. Kilgo PD, Osler TM, Meredith W (2003) The worst injury predicts mortality outcome the best: rethinking the role of multiple injuries in trauma outcome scoring. J Trauma 55:599–606
14. Kilgo PD, Meredith JW, Osler TM (2006) Incorporating recent advances to make the TRISS approach universally available. J Trauma 60:1002–1008
15. Moore L, Lavoie A, Le Sage N et al (2008) Consensus or data-derived anatomic injury severity scoring? J Trauma 64:420–426
16. Holder Y, Peden M, Krug E et al (eds) (2001) Injury Surveillance Guidelines. World Health Organization, Geneva
17. Nakahara S, Jayatilleke AU, Ichikawa M et al (2008) Feasibility of standardized injury surveillance and reporting: a comparison of data from four Asian nations. Inj Prev 14:106–112
18. Japan Trauma Care and Research (2008) Japan Trauma Data Bank Report 2004–2007. http://www.jtcr-jatec.org/traumabank/dataroom/data/JTDB04-07eng.pdf. Accessed 15 September 2010
19. Ichikawa M, Nakahara S, Wakai S (2005) Factors related to participation in the Japan Trauma Data Bank. J Jpn Assoc Acute Med 16:552–556
20. Hosmer DW, Lemeshow S (2000) Applied logistic regression, 2nd edn. Wiley, New York
21. Kimura A (2010) Logistic regression models for Japanese blunt trauma victims: second report. J Jpn Assoc Surg Trauma 24:321–326
22. Kimura A (2010) Logistic regression models for Japanese blunt trauma victims. J Jpn Assoc Surg Trauma 24:15–20
23. Nakahara S, Taira Y, Takahashi M et al. (2008) Extracting information from free-texts in computerized medical records of traffic injury patients admitted to a critical care medical center in Japan. In: Proceedings of the 11th international conference on human and computers, November 20–23, Nagaoka, Japan, pp 215–220
24. Zafar H, Rehmani R, Raja AJ et al (2002) Registry based trauma outcome: perspective of a developing country. Emerg Med J 19:391–394
25. Lane PL, Doig G, Mikrogianakis A et al (1996) An evaluation of Ontario trauma outcomes and the development of regional norms for Trauma and Injury Severity Score (TRISS) analysis. J Trauma 41:731–734
26. Nakahara S, Saint S, Sann S et al (2010) Exploring referral systems for injured patients in low-income countries: a case study from Cambodia. Health Policy Plan 25:319–327
27. DiRusso SM, Sullivan T, Holly C et al (2000) An artificial neural network as a model for prediction of survival in trauma patients: validation for a regional trauma area. J Trauma 49:212–220
28. Schluter PJ, Nathens A, Neal ML et al (2010) Trauma and Injury Severity Score (TRISS) coefficients 2009 revision. J Trauma 68:761–770